OPEN ACCESS

Kashf Journal of Multidisciplinary Research
Vol: 02 - Issue 08 (2025)
P-ISSN: 3007-1992 E-ISSN: 3007-200X
https://kjmr.com.pk

AN IMPLICIT NUMERICAL SCHEME BASED ON B-SPLINE FUNCTIONS FOR TIME -FRACTIONAL BURGERS EQUATION

[1]Manzar Abbas, [2]Muhammad Amin, [3]Ali Usman, [4]Muhammad Waqas*

**[1, 2, 3, 4]Faculty of Sciences, The Superior University Lahore, Pakistan.*

**Corresponding author:* manzarzarkhan123@gmail.com

DOI Url: https://doi.org/10.71146/kjmr572

Article Info

Abstract

This paper focuses on the numerical treatment of the time-fractional Burgers equation, a significant nonlinear partial differential equation with applications in various fields such as fluid dynamics, acoustics and traffic flow. Herein, we propose an Extended Cubic B-Spline ExCBS method for approximating the solution of the time-fractional Burgers equation. The time-fractional derivative is discretized using a finite difference technique while the spatial derivatives are handled by the ExCBS method. The stability and convergence of the proposed scheme are rigorously analyzed. Numerical examples are presented to demonstrate the accuracy and efficiency of the applied method. Comparisons with existing methods in the literature illustrate the superior performance of the proposed technique for solving this class of fractional differential equations. This research offers valuable and effective numerical tool for the investigation of complex phenomena modeled by the time-fractional Burgers equation.

Keywords:

Burgers equation, extended cubic B-Spline method, Caputo Fabrizo derivative, numerical stability, convergence analysis

1. Introduction

Burgers equation is among the most well-known fractional partial differential equations (FPDEs). In recent years, many scientists have shown their interest in solving FPDEs because of their applications in a wide range of scientific and technical fields. A more adaptable model is offered by fractional derivatives, which are also a helpful tool for explaining the variable's past and inherited traits of many dynamical systems. Numerous studies have focused on deriving both analytical and numerical solutions for linear and nonlinear fractional partial differential equations (FPDEs). Among these, Burgers equation stands out as a fundamental nonlinear PDE that encapsulates both nonlinear propagation and diffusive effects. Originally formulated to model the motion of turbulent fluids, Burgers equation exhibits structural similarities to the NavierStokes equations, particularly in terms of its nonlinear terms and the presence of higher-order derivatives with relatively small coefficients. These features contribute to the complexity of modeling turbulent flows. The time-fractional variant of Burgers equation (TFBE) extends the classical form by incorporating a fractional time derivative, which accounts for memory effects often encountered in physical systems. Specifically, the fractional derivative represents the influence of wall friction across the boundary layer, making the equation suitable for modeling phenomena such as the unidirectional propagation of weakly nonlinear acoustic waves in gas-filled ducts. Additionally, the fractional Burgers equation (FBE) finds applications in various fields, including the modeling of bubbly fluids and shallow water waves, as discussed in previous works [1 - 4]

The following is how the one-dimensional time-fractional Burgers equation is seen [5-7]

$$\frac{\partial^{\beta} z(r,t)}{\partial t^{\beta}} + z(r,t)\frac{\partial z(r,t)}{\partial r} - v\frac{\partial^{2} z(r,t)}{\partial r^{2}} = f(r,t), \qquad (r,t) \in [p,q]\times[O,T]. \tag{1}$$

with initial and boundary conditions

$$\begin{cases} z(r,t) = \omega(t), \;\; p \le r \le q \\ z(p,t) = \theta_1(t), \;\; t \ge 0 \\ z(p,t) = \theta_2(t). \end{cases} \tag{2}$$

Where $\beta \in (0,1)$, here v denotes the viscosity parameter ω(t), $\theta_1(t)$, $\theta_2(t)$, and $f(r,t)$ are suitably prescribed boundary function. The Caputo Fabrizio fractional derivative offers an effective framework for modeling diffusion-type processes, particularly due to its non-singular kernel, which facilitates more accurate and efficient numerical treatment of fractional diffusion equations.

The Caputo Fabrizo fractional derivative

$$\frac{\partial^{\beta} z(r,t)}{\partial t^{\beta}} = \frac{R(\beta)}{2-\beta} \int_{o}^{t_{m+1}} \frac{\partial^{2}}{\partial f^{2}} z(r,t) \exp\left[-\frac{\beta}{2-\beta} (t_{m+1} - f) \right] df. \tag{3}$$

Recent studies have highlighted concerns regarding the limitations of power-law kernels commonly employed in fractional differential operators. Specifically, it has been observed that such kernels may inadequately model certain physical phenomena such as fatigue experienced by long-distance runners and non-local behaviors like cross over effects [8-10] To address these limitations, researchers have explored alternative fractional derivatives. Among the most influential contributions is the Caputo fractional derivative, which has gained prominence due to its ability to incorporate conventional initial and boundary conditions naturally within its formulation. For constant functions, the Caputo derivative evaluates to zero, making it particularly useful in physical modeling. In groundwater studies, accurate modeling requires both the drawdown and its derivative to be anchored at a central borehole location. Complementary fractional derivatives can be used to meet this constraint, particularly in situations where the aquifers piezometric head decreases as the distance from the borehole increases. Over time, a wide array of numerical techniques has been developed for solving fractional partial differential equations (FPDEs) [11-13]. A group-preserving approach to fractional Burgers equation (FBE) solution was put forth by Hashemi *et al.* [14]. Akgül introduced the use of Atangana -Baleanu derivatives for both linear and nonlinear instances in the mimicking kernel Hilbert space technique. Later on Momani applied this framework to obtain approximate analytical solutions of the FBE. Further contributions include the Homotopy Analysis method by Song and Zhang, who validated their approach with numerical simulations [15]. Liu and Hou [16] used the extended differential transform method for time and space-fractional versions. Danaf and Handhold [17] developed a computational strategy based on cubic parametric splines to solve the time-fractional Burgers equation. A comprehensive overview of theoretical and numerical results related to FBEs was presented by Lombard *et al.* [18]. Additional advancements include the application of the variational iteration method by Saad and Sharif [19] and the finite difference Chebyshev wavelet technique by Yokus *et al.* [20]. B-Spline-based methods have proven efficiency in approximating solutions to FPDEs due to their ability to maintain high smoothness across knots and adapt to solution behavior. Although a substantial body of research has focused on B-Spline techniques for general FPDEs, applications specific to FBEs remain relatively scarce. Quadratic B-Spline methods for TFBE have been explored by Esen and Tabassam [21]. Atangana *et al.* [22] presented a B-Spline based numerical method for fractional diffusion problems. More recently, Maohyud-Din *et al.* [23] solved time-fractional advection-diffusion equations using the extended cubic B-Spline ExCBS finite difference method. Galamian and Najafi [24] developed an ExCBS formulation within the collocation-based spline (CBS) framework to address linear differential equations. Akram *et al.* [25] proposed several numerical strategies for diffusion and time-fractional telegraph

equations. Yaseen and Abbas [26] adopted the cubic trigonometric B-Spline method to solve the TFBE in the absence of a forcing term. Using extended cubic B spline ExCBS basis functions, the current work presents a novel numerical technique for solving the time-fractional Burgers equation. A key innovation lies in the approximation of the second-order spatial derivative through a linear combination of nearby ExCBS function values [27]. This refined approach offers enhanced accuracy and has, to the best of our knowledge, not been previously applied in this context [28]. Usman *et al.* [29] presented a numerical method using the B-Spline collocation technique to solve the time-fractional advection-diffusion equation. Their study demonstrates the method's efficiency and accuracy in handling complex fractional-order problems. Hassan *et al.* [30] developed a hybrid B-Spline method to numerically analyze the time-fractional diffusion wave equation. The approach proved to be effective in enhancing the accuracy and stability of solutions for fractional-order models. Waqas *et al.* [31] introduced an efficient hybrid B-Spline method for the numerical approximation of time-fractional telegraph equations. The technique demonstrated high accuracy and computational efficiency in solving fractional-order problems.

2. Extended Cubic B-Spline

Let $M \in Z^+$ and $[p,q]$ be the time interval at the equidistant knots is separated into equal subintervals $r_i = r_0 + ih, i \in \mathbf{Z}$ with $h = \frac{q-p}{M}$. At each knot over the specified interval, the extended cubic B-Spline (ExCBS) basis functions can be expressed as:

$$B_i(r,\lambda) = \frac{1}{24h^4}\begin{cases} 4h(1-\lambda)(r-r_{i-2})^3 + 3\lambda(r-r_{i-2})^4, & r \in [r_{i-2}, r_{i-1}], \\ (4-\lambda)h^4 + 12h^3(r-r_{i-1}) + 6h^2(2+\lambda)(r-r_{i-1})^2 & \\ -12h(r-r_{i-1})^3 - 3\lambda(r-r_{i-1})^4, & r \in [r_{i-1}, r_i] \\ (4-\lambda)h^4 + 12h^3(r_{i+1}-r) + 6h^2(2+\lambda)(r_{i+1}-r)^2 & \\ -12h(r_{i+1}-r)^3 \_ 3\lambda(r_{i+1}-r)^4 & r \in [r_i, r_{i+1}] \\ 4h(1-\lambda)(r_{i+2}-r)^3 + 3\lambda(r_{i+2}-r)^4 & r \in [r_{i+1}, r_{i+2}] \\ 0 & otherwise. \end{cases} \quad (4)$$

Where $\lambda \in R$ and $r \in R$ are variables and parameters that are both free parameters. For $\lambda = 0$, the ExCBS becomes simple cubic CBS. A basis is formed over the alleged domain $[p,q]$ by the spline $\{B_{-1}, B_0, ..., B_{M+1}\}$. If $Z(r,t)$ is a sufficiently uniform solution, then the identified interpolating requirement is satisfied by a unique ExCBS $Z(r,t)$.

$$Z(r_i,0) = z(r_i,0) \qquad \forall r_i \in [p,q]$$

$$Z'(p,t) = z'(p,t), Z'(q,t) = z'(q,t) \qquad \forall t \in [o,T].$$

Such that

$$z(r,t)=\sum_{i=-1}^{M+1} d_i(t)B_i(r,\lambda), \tag{5}$$

Where coefficients $d_i(t)$ must be determined by specific constraints and rely on time. For the purpose of simplicity we denote $Z(r_\kappa), Z'(r_\kappa), Z''(r_\kappa)$, by $Z_\kappa, w_\kappa, W_\kappa$ respectively. With approximation and the fundamental functions, we obtain the following relationship

$$Z_\kappa=\sum_{i=\kappa-1}^{\kappa+1} d_i(t)B(r_i,\lambda)=\left(\frac{4-\lambda}{24}\right)d_{\kappa-1}+\left(\frac{8+\lambda}{12}\right)d_\kappa+\left(\frac{4-\lambda}{24}\right)d_{\kappa+1}. \tag{6}$$

$$w_\kappa=\sum_{i=\kappa-1}^{\kappa+1} d_i(t)B^{'}(r_i,\lambda)=\left(\frac{-1}{2h}\right)d_{\kappa-1}+\left(\frac{1}{2h}\right)d_{\kappa+1} \tag{7}$$

$$W_\kappa=\sum_{i=\kappa-1}^{\kappa+1} d_i(t)B^{'}(r_i,\lambda)=\left(\frac{2+\lambda}{2h^2}\right)d_{\kappa-1}+\left(-\frac{2+\lambda}{2h^2}\right)d_{\kappa+1}+\left(\frac{2+\lambda}{2h^2}\right)d_{\kappa+1} \tag{8}$$

The following relations can also be ascertained from the equations above [32]

$$w_j=Z'(r_\kappa,\lambda)=z'(r_\kappa)+\frac{\lambda}{24}h^2z'''(r_\kappa)+\frac{5\lambda^2-10\lambda-16}{2880}h^2z^{(5)}(r_\kappa)+O(h^6), \tag{9}$$

$$W_j=Z''(r_{\ j},\lambda)=\left(1+\frac{\lambda}{2}\right)z''(r_\kappa)+\frac{\lambda^2-4}{48}h^2z^{(4)}(r_\kappa)+O(h^4). \tag{10}$$

Therefore, from (8) and (9) we obtain

$$\left\|w_\kappa-z'(r_\kappa)\right\|_\infty=O(h^2), \tag{11}$$

$$\left\|w_\kappa-z'(r_\kappa)\right\|_\infty=O(h^2), \tag{12}$$

2.1. The development of a new extended cubic B-Spline

To find out NExCBS calculation for $z''(r_\kappa)$, we apply W_κ, $\kappa=1,...,M-1$. Employing Taylor's series to obtain

$$W_{\kappa-1}=\left(1+\frac{\lambda}{2}\right)z''(r_{\kappa-1})+\frac{\lambda^2-4}{48}h^2z^{(4)}(r_{\kappa-1})+O(h^4),=\left(1+\frac{\lambda}{2}\right)z''(r_{\kappa})-\left(1+\frac{\lambda}{2}\right)hz''(r_{\kappa})$$

$$+\frac{\lambda^2+12\lambda+20}{48}h^2z^{(4)}(r_{\kappa})-\frac{(\lambda+2)^2}{48}h^3z^{(5)}(r_{\kappa})+O(h^4).$$

Similarly, we have

$$W_{\kappa+1}=\left(1+\frac{\lambda}{2}\right)z''(r_{\kappa})-\left(1+\frac{\lambda}{2}\right)hz''(r_{\kappa})+\frac{\lambda^2+12\lambda+20}{48}h^2z^{(4)}(r_{\kappa})+\frac{(\lambda+2)^2}{48}h^3z^{(5)}(r_{\kappa})+O(h^4).$$

Let W_{κ} be a linear combination representing the approximation.

$$\tilde{W}_{\kappa}=A_1W_{\kappa}+A_2W_{\kappa-1}+A_3W_{\kappa+1}$$

$$\begin{cases}A_1+A_2+A_3=\dfrac{2}{2+\lambda}\\ -A_2+A_3=0\\ (\lambda^2-4)A_1+(\lambda^2+12\lambda+20)A_2+(\lambda^2+12\lambda+20)A_3=0\end{cases}$$

Where $A_1=\dfrac{\lambda+10}{6(\lambda+2)}, A_2=A_3=\dfrac{2-\lambda}{12(2+\lambda)}$,

$$\tilde{w}=\frac{(2-\lambda)d_{\kappa-2}+4(4+\lambda)d_{\kappa-1}-6(6+\lambda)d_{\kappa}+4(4+\lambda)d_{\kappa+1}+(2-\lambda)d_{\kappa+2}}{24h^2}. \quad (13)$$

To build the new estimation for the second order spatial derivative $z''(r_o)$, we employ a linear combination of function values at four neighboring points, denoted as W_0, W_1, W_2 and W_3.

$$\tilde{w}_0=A_1W_0+A_2W_1+A_3W_2+A_4W_3 \quad (14)$$

$$W_1=\left(1+\frac{\lambda}{2}\right)z''(r_0)+\left(1+\frac{\lambda}{2}\right)hz''(r_0)+\frac{\lambda^2+12\lambda+20}{48}h^2z^{(4)}(r_0)$$

$$+\frac{(\lambda+2)^2}{48}h^3z^{(5)}(r_0)+O(h^4),$$

$$W_2 = \left(1+\frac{\lambda}{2}\right)z''(r_0) + \left(1+\frac{\lambda}{2}\right)hz''(r_0) + \frac{(2+\lambda)(46+\lambda)}{48}h^2 z^{(4)}(r_0) + \frac{(\lambda+2)(14+\lambda)}{24}h^3 z^{(5)}(r_0) + O(h^4),$$

$$W_3 = \left(1+\frac{\lambda}{2}\right)z''(r_0) + 3\left(1+\frac{\lambda}{2}\right)hz''(r_0) + \frac{(2+\lambda)(106+\lambda)}{48}h^2 z^{(4)}(r_0) + \frac{(\lambda+2)(34+\lambda)}{48}h^3 z^{(5)}(r_0) + O(h^4).$$

We obtain four linear equations

$$\begin{cases} A_1 + A_2 + A_3 + A_4 = 1 \\ A_2 + 2A_3 + 3A_4 = 0 \\ (\lambda-2)A_1 + (\lambda+10)A_2 + (\lambda+46)A_3 + (\lambda+106)A_4 = 0 \\ (\lambda+2)A_2 + 2(\lambda+14)A_3 + 3(\lambda+34)A_4 = 0 \end{cases}$$

Hence, we get $A_1 = \frac{14-\lambda}{6(2+\lambda)}, A_2 = \frac{5(\lambda-2)}{12(2+\lambda)}, A_3 = \frac{2-\lambda}{3(2+\lambda)}, A_4 = \frac{\lambda-2}{12(2+\lambda)}.$

Expression (13) turns into the following form

$$\tilde{W}_0 = \frac{2(14-\lambda)d_{-1} + 3(3\lambda-22)d_0 + 8(7-2\lambda)d + 14(\lambda-2)d_2 + 6(2-\lambda)d_3 + (\lambda-2)d_4}{24h^2}. \quad (15)$$

Similarly, for $z''(r_M)$, we haves

$$\tilde{W}_M = \frac{(\lambda-2)d_{M-4} + 6(2-\lambda)d_{M-3} + 14(\lambda-2)d_{M-2} + 8(7-2\lambda)d_{M-1} + 3(3\lambda-22)d_M + 2(14-\lambda)d_{M+1}}{24h^2} \quad (16)$$

3. Time discretization

For the temporal discretization, The Caputo Fabrizo fractional derivative (CFFD) has been utilized. Suppose that $t_m = m\Delta t, m = 0,1,...,M$ where $\Delta t = \frac{T}{M}$ denotes the time step size and $0 = t_0 < t_1 < ... < t_M = T$. The CFFD of time-fractional Burgers Equation is discretized at $t = t_{m+1}$ as

$$\frac{\partial^{\beta} z(r,t)}{\partial t^{\beta}} = \frac{R(\beta)}{2-\beta}\int_{o}^{t_{m+1}} \frac{\partial^2}{\partial f^2} z(r,t)\exp\left[-\frac{\beta}{2-\beta}(t_{m+1}-f)\right]df$$
$$= \frac{R(\beta)}{2-\beta}\sum_{r=0}^{m}\int_{0}^{t_{m+1}} \frac{\partial^2}{\partial f^2} z(r,t)\exp\left[-\frac{\beta}{2-\beta}(t_{m+1}-f)\right]df. \quad (17)$$

Using forward difference approach Eq. (17) becomes.

$$\frac{\partial^{\beta} z(r,t_{m+1})}{\partial t^{\beta}} = \frac{R(\beta)}{2-\beta}\sum_{r=0}^{m}\frac{z(r,t_{r+1})-2z(r,t_r)+z(r,t_{r-1})}{(\Delta t)^2}\times\int_{t_r}^{t_{r+1}}\exp\left[-\frac{\beta}{2-\beta}(t_{m+1}-f)\right]df+\theta_{\Delta t}^{m+1}$$

$$=\frac{R(\beta)}{\beta(\Delta t)^2}\left[1-\exp\left[-\frac{\beta}{2-\beta}\Delta t\right]\right]\sum_{r=0}^{n}\left[z(r,t_{m-r+1})-2z(r,t_{m-r})+z(r,t_{m-r+1})\right]\exp\left(-\frac{\beta}{2-\beta}r\Delta t\right)+\theta_{\Delta t}^{m+1}.$$

Hence

$$\frac{\partial^{\beta}}{\partial t^{\beta}} z(r,t_{r+1}) = \frac{\mu R(\beta)}{\beta(\Delta t)^2}\sum_{r=0}^{n} k_r\left[z(r,t_{m-r+1})-2z(r,t_{m-r})+z(r,t_{m-r+1})\right]+\theta_{\Delta t}^{m+1}. \quad (18)$$

Where, $\lambda = 1-\exp\left(-\frac{\beta}{2-\beta}\Delta t\right)$ and $k_r = \exp\left(-\frac{\beta}{2-\beta}r\Delta t\right)$. Moreover, the truncation error $\theta_{\Delta t}^{m+1}$ is given as $\left|\theta_{\Delta t}^{m+1}\right| \le G(\Delta t)^2$

G never changes. It's easy to verify.

- $k_r > 0 and\ k_0 = 1, r = 0,1,...,m.$
- $k_0 > k_1 > k_2 > ... > k_r, k_r \to 0\ as\ r \to \infty$
- $\sum_{r=0}^{m}(k_r - k_{r+1}) + k_{m+1} = (1-k_1) + \sum_{r=1}^{m-1}(k_r - k_{r+1}) + k_m = 1.$

4. Description of New extended B-Spline Method

Here, we suggest using a numerical approach to solve TFBE 1 and Table 2. Utilizing the $\theta - weighted$ method with Caputo Fabrizio fractional derivative to solve the given problem

$$\frac{\mu R(\beta)}{\beta(\Delta t)^2}\sum_{r=0}^{m} k_r\left[z(r,t_{m-r+1})-2z(r,t_{m-1})+z(r,t_{m\_r})\right]+\theta_{\Delta t}^{m+1},$$
$$=\theta\left[vz_{rr}(r,t_{m+1})-zz_r(r,t_{m+1})\right]+1-\theta\left[vz_{rr}-zz_r(r,t_m)\right]+f(r,m+1). \quad (19)$$

$$\frac{\mu R(\beta)}{\beta(\Delta t)^2}\sum_{r=0}^{m} k_r(z^{m-r+1}-2z^{m-1}+z^{m-r-1})+\theta_{\Delta t}^{m+1} = \theta\left(vz_{rr}^{m+1}-zz_r^{m+1}\right)+(1-\theta)(vz_{rr}^{m}-zz_r^{m})+f_r^{m+1}$$

When $\theta = 1$ Rubin and Graves' method of linearizing the non-linear term.

$$\frac{\mu R(\beta)}{\beta(\Delta t)^2}\sum_{r=0}^{m} k_r(z^{m-r+1} - 2z^{m-1} + z^{m-r-1}) + \theta_{\Delta t}^{m+1} = \left(vz_{rr}^{m+1} - zz_r^{m+1}\right) + f_r^{m+1}$$

$$(zz_r)^{m+1} = z^{m+1}z_r^m + z_r^{m+1} - (zz_r)^m. \tag{20}$$

$$\frac{\mu R(\beta)}{\beta(\Delta t)^2}\sum_{r=0}^{m} k_r(z^{m-r+1} - 2z^{m-1} + z^{m-r-1}) = \left(vz_{rr}^{m+1} - z^{m+1}z_r^n - z^m z_r^{m+1}(zz_r)^m\right) + f_r^{m+1},$$

$$\sum_{r=0}^{m} k_r\left(z^{m-r+1} - 2z^{m-1} + z^{m-r-1}\right) = \frac{\beta(\Delta t)}{\mu R(\beta)}(vz_{rr}^{m+1} - z^{m+1}z_r^m - z_r^{m+1} + (zz_r)^m + f_r^{m+1}. \tag{21}$$

Let $g = \dfrac{\beta(\Delta t)^2}{\mu R(\beta)}$

$$\sum_{r=0}^{n} k_r\left(z^{m-r+1} - 2z^{m-1} + z^{m-r-1}\right) = gvz_{rr}^{m+1} - gz^{m+1}z_r^m - gz^m z_r^{m+1} + g(zz_r) + gf_r^{m+1},$$

$$z^{m+1} - 2z^{m-1} + z^{m-1} + \sum_{r=1}^{m} k_r\left(z^{m-r+1} - 2z^{m-1} + z^{m-r-1}\right) = gvz_{rr}^{m+1} - gz^{m+1}z_r^m - gz^m z_r^{m+1} + g(zz_r) + gf_r^{m+1},$$

$$z^{m+1} - gvz_{rr}^{m+1} + gz^{m+1}z_r^m + gz^m z_r^{m+1} = z^{m-1} - \sum_{r=1}^{m} k_r\left(z^{m-r+1} - 2z^{m-1} + z^{m-r-1}\right) + g(zz_r)^m + gf_r^{m+1},$$

$$z^{m+1} + gz^{m+1}z_r^m + gz^m z_r^{m+1} - gvz_{rr}^{m+1} = z^{m-1} + g(zz_r)^m + gf_r^{m+1} - \sum_{r=1}^{m} k_r\left(z^{m-r+1} - 2z^{m-1} + z^{m-r-1}\right),$$

$$z^{m+1} + g(z^{m+1}z_r^m + z^m z_r^{m+1} - vz_{rr}^{m+1}) = z^{m-1} + g(zz_r)^m + gf_r^{m+1} - \sum_{r=1}^{m} k_r\left(z^{m-r+1} - 2z^{m-1} + z^{m-r-1}\right).$$

Employing the ExCBS approximation along with its corresponding derivatives at the knots, the numerical scheme for solving the time-fractional Burgers equation can be effectively formulated.

$$Z_\kappa^{m+1}+g(w_\kappa^m Z_\kappa^{m+1}+Z_\kappa^m w_\kappa^{m+1}-v\tilde{W}_\kappa^{m+1})$$
$$=Z_\kappa^{m+1}+gZ_\kappa^m w_\kappa^m+gf_j^{m+1}-\sum_{p=0}^{m-1}\left(z^{m-r+1}-2z^{m-1}+z^{m-r-1}\right). \tag{22}$$

$\kappa=1,2,...,M-1$

$$\left(\frac{4-\lambda}{24}\right)d_{\kappa-1}^{m+1}+\left(\frac{8+\lambda}{12}\right)d_\kappa^{m+1}+\left(\frac{4-\lambda}{24}\right)d_{\kappa+1}^{m+1}+r\left(\left(\frac{4-\lambda}{24}\right)d_{-1}^{m+1}+\left(\frac{8+\lambda}{12}\right)d_\kappa^{m+1}+\left(\frac{4-\lambda}{24}\right)d_1^{m+1}\right)w_\kappa^m$$
$$+r\left[z_\kappa^m\left(\left(\frac{-1}{2h}\right)d_{\kappa-1}^{m+1}+\left(\frac{1}{2h}\right)d_{\kappa+1}^{m+1}\right)-\frac{gv}{24h^2}\left((2-\lambda)d_{\kappa-2}^{m+1}+4(4+\lambda)d_{\kappa-1}^{m+1}-6(6+\lambda)d_\kappa^{m+1}+4(4+\lambda)d_{\kappa+1}^{m+1}+(2-\lambda)d_{\kappa+2}^{m+1}\right)\right]$$
$$=\left(\frac{4-\lambda}{24}\right)d_{\kappa-1}^{m+1}+\left(\frac{8+\lambda}{12}\right)d_\kappa^{m+1}+\left(\frac{4-\lambda}{24}\right)d_{\kappa+1}^{m+1}+gf_\kappa^{m+1}+g\left[\left(\frac{4-\lambda}{24}\right)d_{\kappa-1}^0+\left(\frac{8+\lambda}{12}\right)d_\kappa^0+\left(\frac{4-\lambda}{24}\right)d_{\kappa+1}^0\right]+gf_\kappa^{m+1}-$$
$$\sum_{r=1}^m k_r\left[\begin{array}{l}\left(\frac{4-\lambda}{24}\right)d_{\kappa-1}^{m-r+1}+\left(\frac{8+\lambda}{12}\right)d_\kappa^{m-r+1}+\left(\frac{4-\lambda}{24}\right)d_{\kappa+1}^{m-r+1}-2\left(\left(\frac{4-\lambda}{24}\right)d_{\kappa-1}^{m-1}+\left(\frac{8+\lambda}{12}\right)d_\kappa^{m-1}+\left(\frac{4-\lambda}{24}\right)d_{\kappa+1}^{m-1}\right)\\+\left(\frac{4-\lambda}{24}\right)d_\kappa^{m-r-1}+\left(\frac{8+\lambda}{12}\right)d_{\kappa+1}^{m-r-1}+\left(\frac{4-\lambda}{24}\right)d_{\kappa-1}^{m-r-1}\end{array}\right]. \tag{23}$$

$\kappa=0$

$$\left(\frac{4-\lambda}{24}\right)d_{-1}^{m+1}+\left(\frac{8+\lambda}{12}\right)d_0^{m+1}+\left(\frac{4-\lambda}{24}\right)d_1^{m+1}+g\left(\left(\frac{4-\lambda}{24}\right)d_{-1}^{m+1}+\left(\frac{8+\lambda}{12}\right)d_0^{m+1}+\left(\frac{4-\lambda}{24}\right)d_1^{m+1}\right)w_0^m$$
$$-\frac{gv}{24h^2}\left[2(14-\lambda)d_{-1}^{m+1}+3(3\lambda-22)d_o^{m+1}+8(7-2\lambda)d_1^{m+1}+14(\lambda-2)d_2^{m+1}6(2-\lambda)d_3^{m+1}+(\lambda-2)d_4^{m+1}\right]+$$
$$g\left(Z_0^m\left(\left(\frac{-1}{2h}\right)d_{-1}^{m+1}+\left(\frac{1}{2h}\right)d_1^{m+1}\right)\right)=\left(\frac{4-\lambda}{24}\right)d_{-1}^{m+1}+\left(\frac{8+\lambda}{12}\right)d_0^{m+1}+\left(\frac{4-\lambda}{24}\right)d_1^{m+1}+gf_0^{m+1} \tag{24}$$
$$+g\left[\left(\frac{4-\lambda}{24}\right)d_{-1}^0+\left(\frac{8+\lambda}{12}\right)d_0^0+\left(\frac{4-\lambda}{24}\right)d_1^0\right].$$
$$-\sum_{r=1}^m k_r\left[\begin{array}{l}\left(\frac{4-\lambda}{24}\right)d_{-1}^{m-r+1}+\left(\frac{8+\lambda}{12}\right)d_0^{m-r+1}+\left(\frac{4-\lambda}{24}\right)d_1^{m-r+1}-2\left(\left(\frac{4-\lambda}{24}\right)d_{-1}^{m-1}+\left(\frac{8+\lambda}{12}\right)d_0^{m-1}+\left(\frac{4-\lambda}{24}\right)d_1^{m-1}\right)\\+\left(\frac{4-\lambda}{24}\right)d_0^{m-r-1}+\left(\frac{8+\lambda}{12}\right)d_1^{m-r-1}+\left(\frac{4-\lambda}{24}\right)d_{-1}^{m-r-1}\end{array}\right]$$

$\kappa=M$

$$\left(\frac{4-\lambda}{24}\right)d_{M-1}^{m+1}+\left(\frac{8+\lambda}{12}\right)d_M^{m+1}+\left(\frac{4-\lambda}{24}\right)d_{M+1}^{m+1}+r\left(\left(\frac{4-\lambda}{24}\right)d_{M-1}^{m+1}+\left(\frac{8+\lambda}{12}\right)d_M^{m+1}+\left(\frac{4-\lambda}{24}\right)d_1^{m+1}\right)w_M^m$$
$$-\frac{gv}{24h^2}\left[(\lambda-2)d_{M-4}^{m+1}+6(2-\lambda)d_{M-3}^{m+1}+14(\lambda-2)d_{M-2}^{m+1}+8(7-2\lambda)d_{M-1}^{m+1}+3(3\lambda-22)d_M^{m+1}+2(14-\lambda)d_{M+1}^{m+1}\right]$$
$$+g\left(z_M^m\left(\left(\frac{-1}{2h}\right)d_{M-1}^{m+1}+\left(\frac{1}{2h}\right)d_{M+1}^{m+1}\right)\right)$$
$$=\left(\frac{4-\lambda}{24}\right)d_{M-1}^{m+1}+\left(\frac{8+\lambda}{12}\right)d_M^{m+1}+\left(\frac{4-\lambda}{24}\right)d_M^{m+1}+gf_M^{m+1}+g\left[\left(\frac{4-\lambda}{24}\right)d_{M-1}^0+\left(\frac{8+\lambda}{12}\right)d_M^0+\left(\frac{4-\lambda}{24}\right)d_{M+1}^0\right]-$$
$$\sum_{r=1}^m k_r\left[\begin{array}{l}\left(\frac{4-\lambda}{24}\right)d_{M+1}^{m-r+1}+\left(\frac{8+\lambda}{12}\right)d_M^{m-r+1}+\left(\frac{4-\lambda}{24}\right)d_{M+1}^{m-r+1}-2\left(\left(\frac{4-\lambda}{24}\right)d_{M-1}^{m-1}+\left(\frac{8+\lambda}{12}\right)d_M^{m-1}+\left(\frac{4-\lambda}{24}\right)d_{M+1}^{m-1}\right)\\+\left(\frac{4-\lambda}{24}\right)d_M^{m-r-1}+\left(\frac{8+\lambda}{12}\right)d_{M+1}^{m-r-1}+\left(\frac{4-\lambda}{24}\right)d_{M-1}^{m-r-1}\end{array}\right].$$

The boundary conditions yield two additional equations.

$$\left(\frac{4-\lambda}{24}\right)d_{-1}^{m+1}+\left(\frac{8+\lambda}{12}\right)d_{0}^{m+1}+\left(\frac{4-\lambda}{24}\right)d_{1}^{m+1}=\theta_1\left(t^{m+1}\right), \tag{25}$$

$$\left(\frac{4-\lambda}{24}\right)d_{M-1}^{m+1}+\left(\frac{8+\lambda}{12}\right)d_{M}^{m+1}+\left(\frac{4-\lambda}{24}\right)d_{M+1}^{m+1}=\theta_2\left(t^{m+1}\right). \tag{26}$$

As a result, we obtain a system of equations of a certain order $(M+3)\times(M+3)$ which admits a unique solution. Prior to initiating the iterative procedure of the numerical scheme, three additional equations are attained from the given initial conditions.

$$Z'_{\kappa}=\omega'\left(r_{\kappa}\right),\ \kappa=0,1,...M. \tag{27}$$

$$Z_{\kappa}^{0}=\omega\left(r_{\kappa}\right),\ \kappa=0,1,...,M. \tag{28}$$

The above equation yields a linear system of a certain order which can be represented in matrix form as follows:

$$AD^{0}=B. \tag{29}$$

5. Analysis of stability

The Von Neumann method is employed to perform the stability analysis, in this process, the nonlinear term zz_r which is a constant in equation (18), leading to the following expression:

$$Z_{\kappa}^{m+1}+g\mu\left(Z_{r}^{m+1}\right)-gvZ_{rr}^{m+1}=Z_{\kappa}^{m}-\sum_{r=1}^{m}k_r\left(Z^{m-r+p}-2Z^{m-1}+Z^{m-r-p}\right)+gf_{\kappa}^{m+1}. \tag{30}$$

Consider $Z_{\kappa}^{m}=\eta e^{i\alpha h\kappa}$, the solution of the above equation be expressed in the form of a single Fourier mode, where α denotes the amount of modes, g represents the spatial step size, $i=\sqrt{-1}$, we obtain

$$\left[\left(\frac{4-\lambda}{24}-\frac{g\mu}{2h}\right)e^{i\alpha h(\kappa-1)}+\left(\frac{8+\lambda}{12}\right)e^{i\alpha h(\kappa)}+\left(\frac{4-\lambda}{24}+\frac{g\mu}{2h}\right)e^{i\alpha h(\kappa+1)}\right]\eta^{m+1}$$
$$-\frac{g\mu}{24h^2}\begin{bmatrix}(2-\lambda)e^{i\alpha h(\kappa-2)}+4(4+\lambda)e^{i\alpha h(\kappa-1)}-6(6+\lambda)e^{i\alpha h(\kappa)}\\+4(4+\lambda)e^{i\alpha h(\kappa+1)}+(2-\lambda)e^{i\alpha h(\kappa+2)}\end{bmatrix}\eta^{m+1}$$
$$=\left(\left(\frac{4-\lambda}{24}\right)e^{i\alpha h(\kappa-1)}+\left(\frac{8+\lambda}{12}\right)e^{i\alpha h\kappa}+\left(\frac{4-\lambda}{24}\right)e^{i\alpha h(\kappa+1)}\right)\eta^{m+1}$$
$$-\sum_{r=1}^{m}k_r\begin{bmatrix}\left(\frac{4-\lambda}{24}\right)\left(\eta^{m-r+p}-2\eta^{m-1}+\eta^{m-r-p}\right)e^{i\alpha h(\kappa-1)}\\+\left(\frac{8+\lambda}{12}\right)\left(\eta^{m-r+p}-2\eta^{m-1}+\eta^{m-r-p}\right)e^{i\alpha h\kappa}\\+\left(\frac{4-\lambda}{24}\right)\left(\eta^{m-r+p}-2\eta^{m-1}+\eta^{m-r-p}\right)e^{i\alpha h(\kappa+1)}\end{bmatrix}.$$

Dividing by $e^{i\alpha h\kappa}$,

$$\left[\left(\frac{8+\lambda}{12}+\frac{4-\lambda}{12}\cos(\alpha h)\right)+\frac{g\mu\sin(\alpha h)}{h}-\frac{gv}{24h^2}\left(2(2-\lambda)\cos(2\alpha h)+8(4+\lambda)\cos(\alpha h)-6(6+\lambda)\right)\right]\eta^{m+1}$$
$$=\left(\frac{8+\lambda}{12}+\frac{4-\lambda}{12}\cos(\alpha h)\right)\eta^{n-1}-\left(\frac{8+\lambda}{12}+\frac{4-\lambda}{12}\cos(\alpha h)\right)\sum_{r=1}^{m}k_r\left(\eta^{m-r+1}-2\eta^{m-1}+\eta^{m-r-1}\right).$$

$$\Rightarrow\eta^{m+1}=\frac{1}{v_1}\left[\eta^m-\sum_{r=1}^{m}k_r\left(\eta^{m-r+1}-2\eta^{m-1}+\eta^{m-r-1}\right)\right] \tag{31}$$

Where

$$v_1=1+\frac{gv(2-\lambda)\sin^2(\alpha h)+4(4+\lambda)\sin^2\left(\frac{\alpha h}{2}\right)+6\mu ghi\sin(\alpha h)}{6+(\lambda-4)\sin^2\left(\frac{\alpha h}{2}\right)}.$$

Obviously $v_1\geq 1$, for all $\lambda>-2$ and $\lambda\neq -2$.

Proposition 5.1

Let $\eta^m, m=0,1,...,N$ be the equation (31) solution, then we get

$$\left|\eta^m\right|\leq\left|\eta^0\right|,\quad m=0,1,...,N. \tag{32}$$

Proof

We shall apply mathematical induction. By setting $m=0$ in Eq. (31), we obtain the following relationship.

$$\eta^1=\frac{1}{v_1}\eta^0 \Rightarrow \left|\eta^1\right|\le\left|\eta^0\right|;\ v_1\ge 1.$$

Assume that for $m=0,1,...,T\times(N-1), \left|\eta^m\right|\le\left|\eta^0\right|$ is accurate, then we have

$$\left|\eta^{m+1}\right|=\frac{1}{v_1}\left|\eta^m\right|+\frac{1}{v_1}\sum_{r=1}^{m}k_r\left(\left\|\eta^{m-r+1}-2\eta^{m-1}+\eta^{m-r-1}\right\|\right)$$

$$\le\frac{1}{v_1}\left|\eta^0\right|+\frac{1}{v_1}\sum_{r=1}^{m}k_r\left(\left\|\eta^0\right|-\left|2\eta^0\right|+\left|\eta^0\right\|\right)$$

$$\left|\eta^{n+1}\right|\le\frac{1}{v_1}\left|\eta^0\right|\le\left|2\eta^0\right|\le\left|\eta^{0}\right|;\qquad v_1\ge 1.$$

Hence, we have $\left|\eta^{m+1}\right|=\left|Z_\kappa^{m+1}\right|\le\left|\eta^0\right|=\left|Z_\kappa^0\right|$, so that $\left\|Z_\kappa^{m+1}\right\|_2\le\left\|\eta^0\right\|_2$. Consequently the current method is stable by nature.

6. Convergence

Theorem 1

Suppose that $z(r,t)\in C^4\ [p,q], \mathrm{f}\in C^2[p,q]$ and $\Omega=\left[p=r_0,r_1,...,r_M=q\right]$ constitute the uniformly spaced segment of $[p,q]$ having a step size of h. If $\hat{z}(r,t)$ is interpolating the TFBE solution at knots using a unique spline $r_0,...,r_M\in\Omega$, Then there is a constant n_κ independent of g, so that for every $t\ge 0$, we have

$$\left\|H^\kappa\left(z(r,t)-Z(r,t)\right)\right\|_\infty\le m_\kappa h^{4-\kappa},\kappa=0,1,2 \tag{33}$$

Lemma 6.1

The ExCBS set [33] $\{C_{-1},C_0,...,C_{M+1}\}$ describe the inequality

$$\sum_{i=-1}^{M+1}\left|B_i(r,\lambda)\right|\le\frac{7}{4},\quad 0\le r\le 1. \tag{34}$$

Theorem 2

An approximate solution $z(r,t)$ to the exact solution $z(r,t)$ of the time-fractional Burgers equation (TFBE), subject to the given initial and boundary conditions, is assumed to exist. Furthermore, if $f \in C^2[0,1]$ we obtain

$$\left\|z(r.t)-Z(r,t)\right\|_\infty \le Nh^2. \tag{35}$$

Here, f is small for every $t \ge 0$ and N is a non-negative constant does not depend on f .

Proof

Let $\hat{z}(r,t)$ is the solution of the $Z(r,t)$ by applying triangle inequality, we get

$$\left\|z(r,t)-Z(r,t)\right\|_\infty \le \left\|z(r,t)-\hat{Z}(r,t)\right\|_\infty + \left\|\hat{z}(r,t)-Z(r,t)\right\|_\infty . \tag{36}$$

By theorem 1 we have

$$\left\|H^\kappa\left(z\left(r,t\right)-\hat{z}(r,t)\right)\right\|_\infty \le n_\kappa h^{4-\kappa}, \qquad \kappa = 0,1,2 \tag{37}$$

Using inequality (35), we obtain

First, we linearize the nonlinear term zz_r by setting z as a constant μ in Eq. (19). By rearranging the resulting expression, we obtain:

$$Z^{m+1} + g\mu z_r^{m+1} - g\nu z_{rr}^{m+1} = z^{m-1} + g(zz_r)^m + gf_\kappa^{m+1} - \sum_{p=1}^{m-1}\left(z^{m-r+1} - 2z^{m-1} + z^{m-r-1}\right).$$

The suggested plan has the following collocation requirement. $Lz(r_\kappa,t) = LZ(r_\kappa,t) = f(r_\kappa,t), \qquad \kappa = 0,1,...,M$. Now, consider that $L\hat{z}(r_\kappa,t) = f(r_\kappa,t)$ and difference form of the suggested plan at any given time level n, $L\left(\hat{z}(r_\kappa,t)-Z(r_\kappa,t)\right)$, can be described,

$$\begin{aligned}
&\left(\frac{4-\lambda}{24}\right)\zeta_{\kappa-1}^{m+1} + \left(\frac{8+\lambda}{12}\right)\zeta_\kappa^{m+1} + \left(\frac{4-\lambda}{24}\right)\zeta_{\kappa+1}^{m+1} + \frac{g\mu}{2h}\left(-\zeta_{\kappa-1}^{m+1} + \zeta_{\kappa+1}^{m+1}\right)\\
&-\frac{g\nu}{24h^2}\left[(2-\lambda)\zeta_{\kappa-2}^{m+1} + 4(4+\lambda)\zeta_{\kappa-1}^{m+1} - 6(6+\lambda)\zeta_\kappa^{m+1} + 4(4+\lambda)\zeta_{\kappa+1}^{m+1} + (2-\lambda)\zeta_{\kappa+2}^{m+1}\right]\\
&= \left(\frac{4-\lambda}{24}\right)\zeta_{\kappa-1}^{m+1} + \left(\frac{8+\lambda}{12}\right)\zeta_\kappa^{m+1} + \left(\frac{4-\lambda}{24}\right)\zeta_{\kappa+1}^{m+1} + gf_\kappa^{m+1} + g\left[\left(\frac{4-\lambda}{24}\right)\zeta_{\kappa-1}^{0} + \left(\frac{8+\lambda}{12}\right)\zeta_\kappa^{0} + \left(\frac{4-\lambda}{24}\right)\zeta_{\kappa+1}^{0}\right]\\
&-\sum_{r=1}^{m} k_r \left[\begin{array}{l}\left(\frac{4-\lambda}{24}\right)\zeta_{\kappa-1}^{m-r+1} + \left(\frac{8+\lambda}{12}\right)\zeta_\kappa^{m-r+1} + \left(\frac{4-\lambda}{24}\right)\zeta_{\kappa+1}^{m-r+1} - 2\left(\left(\frac{4-\lambda}{24}\right)\zeta_{\kappa-1}^{m-1} + \left(\frac{8+\lambda}{12}\right)\zeta_\kappa^{m-1} + \left(\frac{4-\lambda}{24}\right)\zeta_{\kappa+1}^{m-1}\right)\\ + \left(\frac{4-\lambda}{24}\right)\zeta_\kappa^{m-r-1} + \left(\frac{8+\lambda}{12}\right)\zeta_{\kappa+1}^{m-r-1} + \left(\frac{4-\lambda}{24}\right)\zeta_{\kappa-1}^{m-r-1}\end{array}\right].
\end{aligned} \tag{38}$$

For κ =0, we obtain

$$\begin{aligned}
&\left(\frac{4-\lambda}{24}\right)\zeta_{-1}^{m+1}+\left(\frac{8+\lambda}{12}\right)\zeta_{0}^{m+1}+\left(\frac{4-\lambda}{24}\right)\zeta_{1}^{m+1}+\frac{g\mu}{2h}\left(-\zeta_{-1}^{m+1}+\zeta_{1}^{m+1}\right)\\
&-\frac{gv}{24h^2}\left[2(14-\lambda)\zeta_{-1}^{m+1}+3(3\lambda-22)\zeta_{0}^{m+1}+8(7-2\lambda)\zeta_{1}^{m+1}+14(\lambda-2)\zeta_{2}^{m+1}+6(2-\lambda)\zeta_{3}^{m+1}+(\lambda-2)\zeta_{4}^{m+1}\right]\\
&=\left(\frac{4-\lambda}{24}\right)\zeta_{-1}^{m+1}+\left(\frac{8+\lambda}{12}\right)\zeta_{0}^{m+1}+\left(\frac{4-\lambda}{24}\right)\zeta_{1}^{m+1}+gf_{\kappa}^{m+1}+g\left[\left(\frac{4-\lambda}{24}\right)\zeta_{-1}^{0}+\left(\frac{8+\lambda}{12}\right)\zeta_{0}^{m}+\left(\frac{4-\lambda}{24}\right)\zeta_{1}^{0}\right]\\
&-\sum_{r=1}^{m}k_r\left[\begin{array}{l}\left(\frac{4-\lambda}{24}\right)\zeta_{-1}^{m-r+1}+\left(\frac{8+\lambda}{12}\right)\zeta_{0}^{m-r+1}+\left(\frac{4-\lambda}{24}\right)\zeta_{1}^{m-r+1}-2\left(\left(\frac{4-\lambda}{24}\right)\zeta_{-1}^{m-1}+\left(\frac{8+\lambda}{12}\right)\zeta_{0}^{m-1}+\left(\frac{4-\lambda}{24}\right)\zeta_{1}^{m-1}\right)\\+\left(\frac{4-\lambda}{24}\right)\zeta_{0}^{m-r-1}+\left(\frac{8+\lambda}{12}\right)\zeta_{1}^{m-r-1}+\left(\frac{4-\lambda}{24}\right)\zeta_{-1}^{m-r-1}\end{array}\right].
\end{aligned}\tag{39}$$

For κ =M

$$\begin{aligned}
&\left(\frac{4-\lambda}{24}\right)\zeta_{M-1}^{m+1}+\left(\frac{8+\lambda}{12}\right)\zeta_{M}^{m+1}+\left(\frac{4-\lambda}{24}\right)\zeta_{M+1}^{m+1}+\frac{g\mu}{2h}\left(-\zeta_{M-1}^{m+1}+\zeta_{M+1}^{m+1}\right)\\
&-\frac{gv}{24h^2}\left[\begin{array}{l}2(14-\lambda)\zeta_{M-1}^{m+1}+3(3\lambda-22)\zeta_{M}^{m+1}+8(7-2\lambda)\zeta_{M+1}^{m+1}+14(\lambda-2)\zeta_{M+2}^{m+1}\\+6(2-\lambda)\zeta_{M+3}^{m+1}+(\lambda-2)\zeta_{M+4}^{m+1}\end{array}\right]\\
&=\left(\frac{4-\lambda}{24}\right)\zeta_{M-1}^{m+1}+\left(\frac{8+\lambda}{12}\right)\zeta_{M}^{m+1}+\left(\frac{4-\lambda}{24}\right)\zeta_{M+1}^{m+1}+gf_{M}^{m+1}\\
&+g\left[\left(\frac{4-\lambda}{24}\right)\zeta_{M-1}^{0}+\left(\frac{8+\lambda}{12}\right)\zeta_{M}^{0}+\left(\frac{4-\lambda}{24}\right)\zeta_{M+1}^{0}\right]\\
&-\sum_{r=1}^{m}k_r\left[\begin{array}{l}\left(\frac{4-\lambda}{24}\right)\zeta_{M-1}^{m-r+1}+\left(\frac{8+\lambda}{12}\right)\zeta_{M}^{m-r+1}+\left(\frac{4-\lambda}{24}\right)\zeta_{M+1}^{m-r+1}\\-2\left(\left(\frac{4-\lambda}{24}\right)\zeta_{M-1}^{m-1}+\left(\frac{8+\lambda}{12}\right)\zeta_{M}^{m-1}+\left(\frac{4-\lambda}{24}\right)\zeta_{M+1}^{m-1}\right)\\+\left(\frac{4-\lambda}{24}\right)\zeta_{M}^{m-r-1}+\left(\frac{8+\lambda}{12}\right)\zeta_{M+1}^{m-r-1}+\left(\frac{4-\lambda}{24}\right)\zeta_{n-1}^{m-r-1}\end{array}\right].
\end{aligned}$$

From the boundary conditions for κ =0, M

$$\begin{aligned}
&\left(\frac{4-\lambda}{24}\right)\zeta_{-1}^{m+1}+\left(\frac{8+\lambda}{12}\right)\zeta_{0}^{m+1}+\left(\frac{4-\lambda}{24}\right)\zeta_{1}^{m+1}=0,\\
&\left(\frac{4-\lambda}{24}\right)\zeta_{M-1}^{m+1}+\left(\frac{8+\lambda}{12}\right)\zeta_{M}^{m+1}+\left(\frac{4-\lambda}{24}\right)\zeta_{m+1}^{m+1}=0.
\end{aligned}$$

Here ζ is as,

$$\zeta_{\kappa}=d_{\kappa}^{m}-c_{\kappa}^{m},\qquad \kappa=0,1,...,M+1\tag{40}$$

Consequently, we have

$$g_\kappa^m = h^2\left[f_\kappa^m - \hat{f}_\kappa^m\right] \le nh^4, \qquad \kappa = 0,1,...,M. \tag{41}$$

Examine $g^m = \max\left\{\left|g_\kappa^m\right|; 0 \le \kappa \le M\right\}, e_\kappa^m = \left|\zeta_\kappa^m\right| and\ e^m = \max\left\{\left|e_\kappa^m\right|; 0 \le \kappa \le M\right\}$. Putting $n = 0$ in Eq. (38), we have

$$\left(\frac{8+\lambda}{12} + \frac{gv(6+\lambda)}{4h^2}\right)\zeta_\kappa^1 = -\left(\frac{4-\lambda}{24} - \frac{gv}{24h^2}4(4+\lambda)\right)(\zeta_{\kappa-1}^1 + \zeta_{\kappa+1}^1) - \frac{gv}{2h}(\zeta_{\kappa-1}^1 + \zeta_{\kappa+1}^1) +$$
$$\frac{gv}{24h^2}(2-\lambda)\times(\zeta_{\kappa-2}^1 + \zeta_{\kappa+2}^1) + \frac{4-\lambda}{24}\zeta_{\kappa-1}^0 + \frac{8+\lambda}{12}\zeta_\kappa^0 + \frac{4-\lambda}{24}\zeta_{\kappa+1}^0 + gf_\kappa^1, \quad \kappa = 1,2,...,M-1$$

Using the values of $g_\kappa^1, \zeta_\kappa^1$ based on the initial condition $e^0 = 0$. we obtain the following expression, and thus the above equation becomes:

$$e_\kappa^1 \le \frac{6ngh^4}{h^2(2+\lambda) + 4gv(4+\lambda) - 6g\mu h}, \quad \kappa = 1,2,...,M-1$$
$$\left(\frac{8+\lambda}{12} + \frac{gv(6+\lambda)}{4h^2}\right)\zeta_0^1 = -\left(\frac{4-\lambda}{24} - \frac{gv}{24h^2}2(14-\lambda)\right)\zeta_{-1}^1$$
$$-\left(\frac{4-\lambda}{24} - \frac{gv}{24h^2}8(7-2\lambda)\right)\zeta_1^1 - \frac{g\mu}{2h}(-\zeta_{-1}^1 + \zeta_1^1)$$
$$+\frac{gv}{24h^2}\left[14(\lambda-2)\zeta_2^1 + 6(2-\lambda)\zeta_3^1 + (\lambda-2)\zeta_4^1\right]$$
$$+\frac{4-\lambda}{24}\zeta_{-1}^0 + \frac{8+\lambda}{12}\zeta_0^0 + \frac{4-\lambda}{24}\zeta_1^0 + \frac{1}{h^2}g_0^1.$$

Taking absolute values of values of $g_0^1 and\ \zeta_0^1$, we have

$$e_0^1 \le \frac{24gnh^4}{4h^2(2+\lambda) + 15gv(\lambda-2) - 24g\mu} \tag{42}$$

Likewise, for $\kappa = M$, we have

$$e_M^1 \le \frac{24gnh^4}{4h^2(2+\lambda) + 15gv(\lambda-2) - 24g\mu} \tag{43}$$

Form the boundary conditions, we obtain

$$e_{-1}^1 \le nh^2,\ e_{M+1}^1 \le nh^2$$

Which implies

$$e^1 \le n_1 h^2. \tag{44}$$

Here n_1 is independent of the spatial step size h. To establish this result, mathematical induction is employed. Let for $l=0,1,2,...,M$, e_κ^1 holds and $n=\max_{0\le l\le m} n_{l,}$ then we get Eq. (38)

$$e_\kappa^{m+1} \le \frac{6nh^4(g-\sum_{r=1}^{m} k_r(z^{m-r+1}-2z^{m-1}+z^{m-r-1})}{h^2(2+\lambda)+4gv(4+\lambda)-6g\mu h}.$$

Similarly, from Eq. (41), (42) we obtain

$$e_0^{m+1} \le nh^2, e_M^{n+1} \le nh^2, e_{-1}^{m+1} \le nh^2, e_{M+1}^{m+1} \le nh^2,$$

Here m is always independent of h,

$$e^{m+1} \le nh^2. \tag{45}$$

Now from above inequality and Lemma

$$\hat{z}(r,t)-Z(r,t)=\sum_{\kappa=-1}^{M+1}(d_\kappa(t)-c_\kappa(t))B_\kappa(r,\lambda). \tag{46}$$

Therefore,

$$\left\|\hat{z}(r,t)-Z(r,t)\right\|_\infty \le \frac{7}{4}nh^2. \tag{47}$$

Here, from inequality (39) we get,

$$\left\|z(r,t)-\hat{z}(r,t)\right\|_\infty+\left\|\hat{z}(r,t)-Z(r,t)\right\|_\infty \le n_0h^4+\frac{7}{4}nh^2=Ch^2. \tag{48}$$

Where $D=n_0h^2+\frac{7}{4}n.$ Hence for every n there exists a positive m independent of h.

Theorem3 The problem along with the initial & boundary conditions is convergent.

Proof

Consider $z(r,t)$ be the approximated solution and exact solution of given problem is defined as $Z(r,t)$.Thus above theorem and expression (19) which demonstrate that there are arbitrary constants M and G such that

$$\left\|z(r.t)-Z(r,t)\right\|_\infty \le Mh^2+G\lambda^{2-\beta}$$

Thus, proposed scheme is convergent.

7. Numerical Results

The E_X CBS method's new approximation yields a numerical solution. To verify the new approximation's accuracy, the $\|e\|_\infty$, and $\|e\|_2$ norms. The outcomes of the new approximation are in good agreement with the precise figures. The computed norms $\|e\|_\infty, and \|e\|_2$ are explained as under:

$$\|e\|_\infty = \left\|z\left(r_\kappa,t\right)-Z\left(r_\kappa,t\right)\right\|_\infty = \max_{o\le\kappa\le M}\left|z\left(r_\kappa,t\right)-Z\left(r_\kappa,t\right)\right|,$$

By definition of Order of convergence [34],

$$Order = \frac{\log\left(\|e\|_\infty\left(M_i\right)\right)-\log\left(\|e\|_\infty\left(M_{i+1}\right)\right)}{\log\left(M_{\kappa+1}\right)-\log\left(M_i\right)},$$

where absolute errors $\|e\|_\infty\left(M_i\right), and, \|e\|_\infty\left(M_{i+1}\right)$ for number of partitioning respectively.

Example 1: Consider the test problem [7] given in (1) subject to the following s conditions:

$$\frac{\partial^\beta z(r,t)}{\partial t^\beta}+z(r,t)\frac{\partial z(r,t)}{\partial r}-v\frac{\partial^2 z(r,t)}{\partial r^2}=f(r,t), \quad (r,t)\in[p,q]\times[O,T].$$

$$\begin{cases} z\left(r,0\right)=0, & 0\le r\le 1 \\ z\left(0,t\right)=t^2, & t\ge 0 \\ z\left(1,t\right)=et^2. \end{cases}$$

Where $f\left(r,t\right)=\frac{2t^{2-\beta}e^r}{\Gamma\left(3-\beta\right)}+t^4e^{2r}-vt^2e^r$ and exact solution $z\left(r,t\right)=t^2e^r$, for all $\left(r,t\right)\in[0,1]\times[0,1]$. Here we choose v=1, T=1

The generic equation, (4) can be written as;

$$Z\left(r,t\right)=d^m_{\kappa-1}B_{\kappa-1}\left(r,\lambda\right)+d^m_\kappa B_\kappa\left(r,\lambda\right)+d^n_{\kappa+1}B_{\kappa+1}\left(r,\lambda\right)$$

Table1 presents a comparative analysis of the norms $\|e\|_\infty, \|e\|_2$ at different values of N when $\beta=0.5, \Delta t=0.00025$ and $T=1$. The results clearly indicate that the suggested method provides significantly lower errors norms compared to the method in [6]. As the number of grid points increases, the norms decrease. Table 2 shows comparison of the errors at different values of Δt with $\beta=0.5$ and $N=80$. Table3 indicates the exact and approximate

errors at different values of r when $\beta = 0.75$ and $N = 40$. The results show that the approximate values are very close to the exact solutions Table depicts 4 the exact and approximate errors at different values of r when $\Delta t = 0.01, N = 40$. ssTable5 shows the exact and approximate errors at different values of r when $\Delta t = 0.01$ and $N = 500$. *Figure 1* and Figure 2 represents a 3D plot for the exact and the approximate solutions when $N = 40, \beta = 0.4$ and $\Delta t = 0.01$. Figure 2 shows a 2D Plot for the exact and approximate solutions of Example 1 with $N = 40, \beta = 0.4$ and $\Delta t = 0.01$. Figure 3 Absolute error for Example 1 with $N = 40, \beta = 0.4$ and $\Delta t = 0.01$.

Table 1 Comparison of the error norms for Example 1 at different values of N when $\beta = 0.5$, $\Delta t = 0.00025$, and $T = 1$

N	Method in [6]		Presented Method		
	$\|e\|_{\infty}$	$\|e\|_{2}$	$\|e\|_{\infty}$	$\|e\|_{2}$	Place the order
10	2.298×10^{-4}	1.634×10^{-4}	2.4307×10^{-6}	1.3941×10^{-6}	……..
20	5.302×10^{-4}	4.477×10^{-4}	5.0813×10^{-7}	4.3203×10^{-7}	2.1022
40	2.275×10^{-4}	1.618×10^{-4}	2.9613×10^{-7}	1.3848×10^{-7}	1.9918
80	1.331×10^{-4}	9.262×10^{-4}	3.2517×10^{-8}	2.4091×10^{-8}	2.5232

Table 2 Comparison of the error norms for Example 1 at different values of Δt when $\beta = 0.5$, and $N = 80$.

Δt	Method [6]		Presented Method		
	$\|e\|_{\infty}$	$\|e\|_{2}$	$\|e\|_{\infty}$	$\|e\|_{2}$	Place the order
0.002	9.368×10^{-4}	6.609×10^{-4}	2.0135×10^{-5}	7.9212×10^{-6}	……..
0.001	5.302×10^{-4}	3.750×10^{-4}	4.3721×10^{-5}	3.9245×10^{-6}	1.9915
0.0005	3.283×10^{-4}	2.328×10^{-4}	2.1745×10^{-7}	1.0912×10^{-7}	2.0054
0.00025	1.331×10^{-4}	9.262×10^{-4}	3.8407×10^{-8}	2.2114×10^{-8}	2.7152

Table 3 The exact and approximate error for the Example 1 at different values of r when $\beta = 0.75$ and N=40.

r	Exact solution	Approximate solution	Error
0.0	1	1	2.2043×10^{-12}
0.1	1.01005	1.01005	4.79315×10^{-6}
0.2	1.02020	1.02021	9.54871×10^{-6}
0.3	1.03046	1.03048	1.42665×10^{-5}
0.4	1.04081	1.04083	1.89458×10^{-5}
0.5	1.05127	1.05129	2.35868×10^{-5}
0.6	1.06184	1.06186	2.8188×10^{-5}
0.7	1.07251	1.07254	3.27515×10^{-5}
0.8	1.08329	1.08332	3.372745×10^{-5}
0.9	1.09636	1.09422	4.7574×10^{-5}
1.0	1.10517	1.10522	4.61996×10^{-5}

Table 4 The exact and approximate numerical solutions for Example 1 at different values of r when N=40 and $\Delta t = 0.01$.

r	Exact solution	Approximate solution	Error
0.0	1	1	3.292992×10^{-13}
0.1	1.10517	1.10542	2.52211×10^{-4}
0.2	1.2214	1.22188	4.77398×10^{-6}
0.3	1.34986	1.35053	6.70325×10^{-4}
0.4	1.49182	1.49265	8.24312×10^{-4}
0.5	1.64872	1.64965	9.30378×10^{-4}
0.6	1.82212	1.73421	9.75590×10^{-4}
0.7	2.01375	2.0147	9.42443×10^{-4}

0.8	2.22554	2.22634	8.02104×10^{-4}
0.9	2.4596	2.39948	6.01369×10^{-4}
1.0	2.71828	2.71828	8.01369×10^{-4}

Table 5 Computation of exact and approximate solutions for Example 1 across various values of r when N=40 and $\Delta t = 0.01$.

r	Exact solution	Approximate solution	Error
0.0	1	1	8.9484×10^{-14}
0.1	1.01005	1.00803	2.26387×10^{-6}
0.2	1.02202	1.02021	5.3734×10^{-6}
0.3	1.03045	1.03253	8.03843×10^{-5}
0.4	1.04081	1.04082	1.06888×10^{-5}
0.5	1.05127	1.05128	1.33243×10^{-5}
0.6	1.06184	1.06185	1.59448×10^{-5}
0.7	1.07251	1.07253	1.85501×10^{-5}
0.8	1.08329	1.08331	2.11399×10^{-5}
0.9	1.09417	1.09201	2.3714×10^{-5}

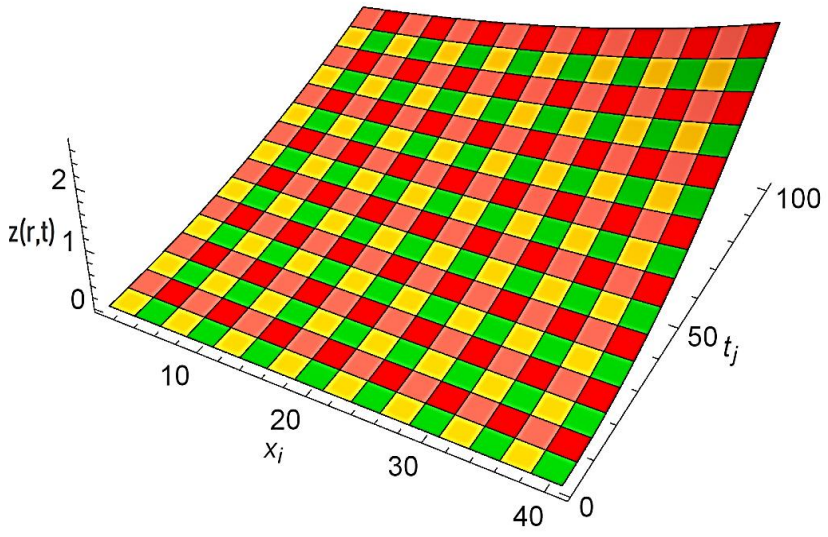

Figure 1 3D plot for the exact solution when $N = 40, \beta = 0.4$ ***and*** $\Delta t = 0.01$**.**

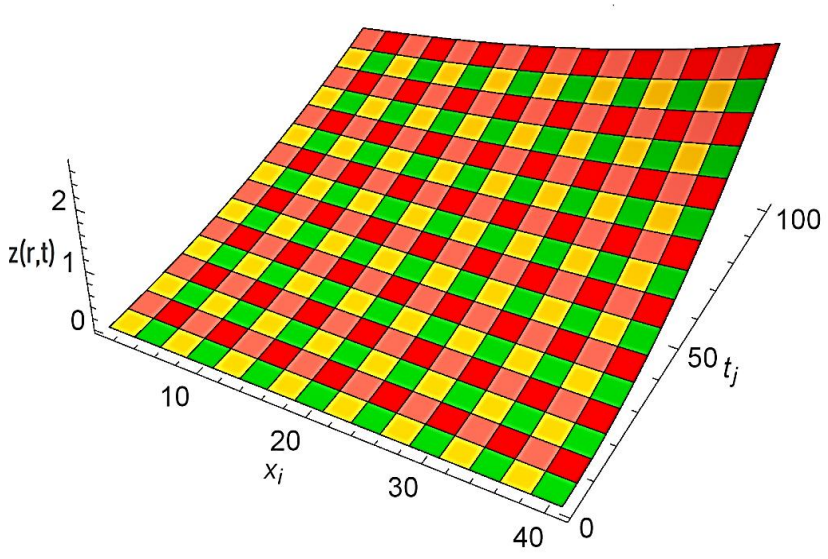

Figure 2 3D plot for the approximated solutions $N = 40, \beta = 0.4$ ***and*** $\Delta t = 0.01$**.**

Piecewise Approximate solution to Example 1, with N=40, h=0.05, **r ∈ [0, 1]**

$$Z(r,t)=\begin{cases}0+1.99755r-0.0678002r^2+1.27486r^3-6.53819r^4, & r\in[0.00,0.05)\\ -0.0342878+\mathrm{r}\left(2.69241+\mathrm{r}\left(-5.00088+\mathrm{r}\left(14.9865-16.8619r\right)\right)\right), & r\in[0.05,\ 0.10)\\ -0.574777+\mathrm{r}\left(8.18874+\mathrm{r}\left(-24.6292+\mathrm{r}\left(42.602-27.6673r\right)\right)\right), & r\in[0.10,\ 0.15)\\ -3.23162+\mathrm{r}\left(26.1605+\mathrm{r}\left(-67.2557+\mathrm{r}\left(82.2807-37.7754r\right)\right)\right), & r\in[0.15,\ 0.20)\\ -11.286+\mathrm{r}\left(66.894+\mathrm{r}\left(-139.332+\mathrm{r}\left(132.052-46.9535r\right)\right)\right), & r\in[0.20,\ 0.25)\\ -29.9021+\mathrm{r}\left(141.889+\mathrm{r}\left(-244.715+\mathrm{r}\left(189.379-54.9755r\right)\right)\right), & r\in[0.25,\ 0.30)\\ -65.9335+\mathrm{r}\left(262.163+\mathrm{r}\left(-384.176+\mathrm{r}\left(251.272-61.6438r\right)\right)\right), & r\in[0.30,\ 0.35)\\ -127.276+\mathrm{r}\left(436.374+\mathrm{r}\left(-555.069+\mathrm{r}\left(314.406-66.7943r\right)\right)\right), & r\in[0.35,\ 0.40)\\ -222.76+\mathrm{r}\left(668.895+\mathrm{r}\left(-751.174+\mathrm{r}\left(375.235-70.2999r\right)\right)\right), & r\in[0.40,\ 0.45)\\ -355.633+\mathrm{r}\left(957.997+\mathrm{r}\left(-962.765+\mathrm{r}\left(430.143-72.0747r\right)\right)\right), & r\in[0.45,\ 0.50)\\ -531.716+\mathrm{r}\left(1294.29+\mathrm{r}\left(-1176.86+\mathrm{r}\left(475.574-72.0747r\right)\right)\right), & r\in[0.50,\ 0.55)\\ -747.378+\mathrm{r}\left(1659.57+\mathrm{r}\left(-1377.67+\mathrm{r}\left(508.18-70.2999r\right)\right)\right), & r\in[0.55,\ 0.60)\\ -992.5+\mathrm{r}\left(2026.22+\mathrm{r}\left(-1547.27+\mathrm{r}\left(524.956-66.7942r\right)\right)\right), & r\in[0.60,\ 0.65)\\ -1247.63+\mathrm{r}\left(2357.18+\mathrm{r}\left(-1666.39+\mathrm{r}\left(523.366-61.6438r\right)\right)\right), & r\in[0.65,\ 0.70)\\ -1482.57+\mathrm{r}\left(2606.76+\mathrm{r}\left(-1715.38+\mathrm{r}\left(501.464-54.9755r\right)\right)\right), & r\in[0.70,\ 0.75)\\ -1655.54+\mathrm{r}\left(2722.07+\mathrm{r}\left(-1675.25+\mathrm{r}\left(457.983-46.9535r\right)\right)\right), & r\in[0.75,\ 0.80)\\ -1713.28+\mathrm{r}\left(2645.28+\mathrm{r}\left(-1528.75+\mathrm{r}\left(392.418-37.7754r\right)\right)\right), & r\in[0.80,\ 0.85)\\ -1592.05+\mathrm{r}\left(2316.61+\mathrm{r}\left(-1261.51+\mathrm{r}\left(305.076-27.6673r\right)\right)\right), & r\in[0.85,\ 0.90)\\ -1218.76+\mathrm{r}\left(1676.3+\mathrm{r}\left(-862.279+\mathrm{r}\left(196.907-16.8619r\right)\right)\right), & r\in[0.90,\ 0.95)\\ -591.744+\mathrm{r}\left(771.58+\mathrm{r}\left(-375.228+\mathrm{r}\left(80.8864-6.53819r\right)\right)\right), & r\in[0.95,\ 1.00].\end{cases}$$

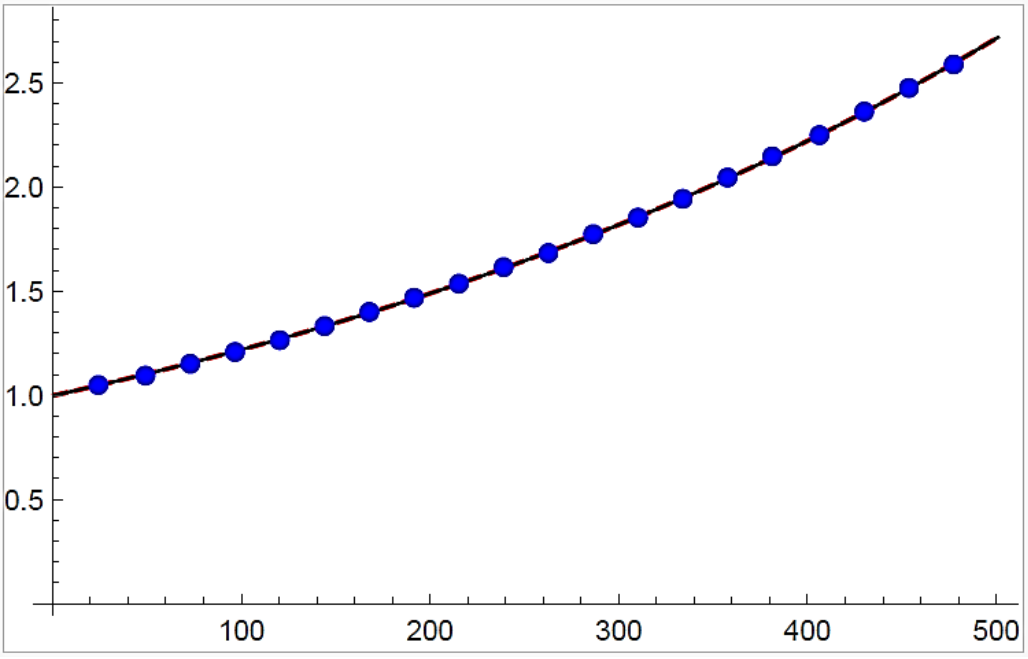

Figure 3 2D Plot for the exact and approximate solutions of Example 1 with $N = 40, \beta = 0.4$ **and** $\Delta t = 0.01$**.**

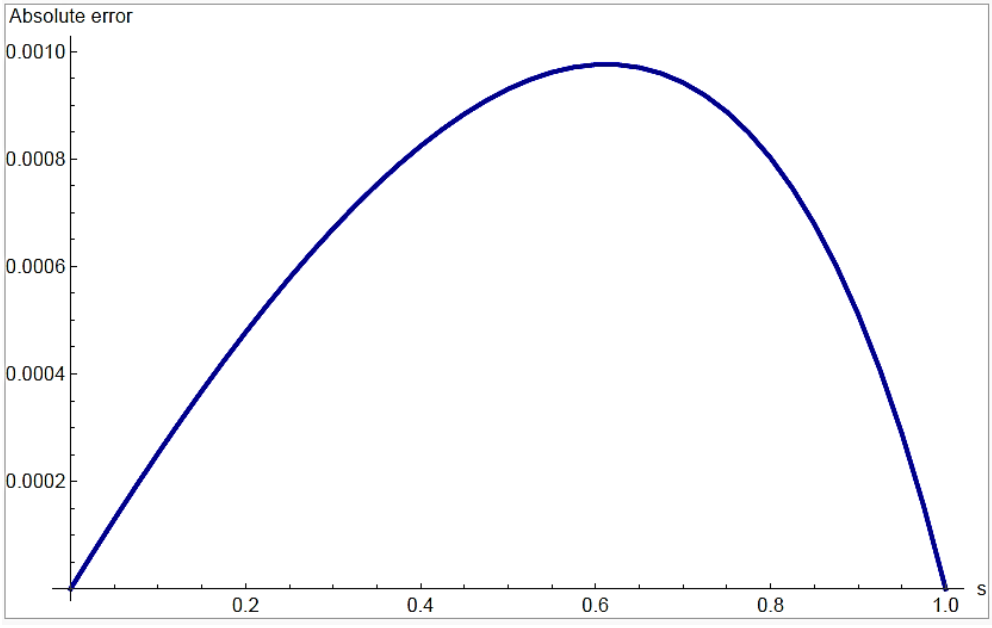

Figure 4 Absolute error for Example 1 with $N = 40, \beta = 0.4$ **and** $\Delta t = 0.01$**.**

Example 2: Consider the following time-fractional Burgers Equation

$$f(r,t)=\frac{2t^{2-\beta}\cos(\pi r)}{\Gamma(3-\beta)}-\pi t^{4}\cos(\pi r)\sin\pi r+v\pi^{2}t^{2}\times\cos(\pi r)$$

The end conditions are

$$\begin{cases} z(r,0)=0, & 0\le r\le 1 \\ z(0,t)=t^{2}, & t\ge 0 \\ z(1,t)=-t^{2} \end{cases}$$

Table 6 display evaluation of errors at different value of r when $N=80$, $T=0.1$ and $\Delta t=0.00025$. In every case, the proposed method yields considerably lower errors, indicating a clear improvement in accuracy .Table 7 shows comparison of the norms at different values of β when $N=80$, $T=1$ and $\Delta t=0.00025$ .In all cases, the proposed method gives much smaller errors. This shows the proposed method is consistently more accurate across all β values. The table 8 indicate the exact and approximate errors at different values of r we take T = 1, N = 100 and $\Delta t=0.001$.The errors are larger at very low r values, reach their minimum around $r=0.5$,and then increase again as r approaches 1.0. Among the tested cases , $\beta=0.7$ often produces the lowest errors, suggesting it offers better accuracy in multiple ranges. This pattern indicates that both r and β significantly influence the precision of the results, and certain combinations yield exceptionally small errors. Figure 5and 6 represent a 3D plot the exact and approximated solution when $N=40,\beta=0.4$ and $\Delta t=0.01$ Figure 7 absolute error for example 2 with $N=40,\beta=0.4$ and $\Delta t=0.01$.

Table 6 Comparison of the error norms for Example 2 at different values of r when

$N=80,T=1,$ *and* $\Delta t=0.00025$

r	Method in [6]		Proposed Method	
-	$\|e\|_{\infty}$	$\|e\|_{2.}$	$\|e\|_{\infty.}$	$\|e\|_{2.}$
0.1	9.009×10^{-6}	6.442×10^{-6}	2.3291×10^{-9}	1.3583×10^{-10}
0.5	8.167×10^{-6}	5.834×10^{-6}	5.2409×10^{-9}	4.2012×10^{-10}
1.0	4.426×10^{-6}	3.117×10^{-6}	7.0198×10^{-8}	3.773810^{-7}

Table 7 Comparison of the error norms for Example 2 at different values of β when

$N = 80, T = 0.1, \Delta t = 0.00025$

	Method in [6]		Proposed Method	
β	$\|e\|_\infty$	$\|e\|_2$	$\|e\|_\infty$	$\|e\|_2$
0.10	6.456×10^{-6}	3.493×10^{-6}	8.5213×10^{-7}	7.1208×10^{-7}
0.25	5.258×10^{-6}	2.738×10^{-6}	6.0982×10^{-7}	5.0083×10^{-7}
0.75	3.445×10^{-6}	1.522×10^{-6}	3.2072×10^{-7}	2.5149×10^{-7}
0.90	4.066×10^{-6}	1.887×10^{-6}	2.1948×10^{-7}	1.0395×10^{-7}

Table 8 The exact and approximate error for Example 2 at different values of r when

$N = 100, \Delta t = 0.001$

	N E_X CBS			
r	$\beta = 0.1$	$\beta = 0.3$	$\beta = 0.7$	$\beta = 0.9$
0.1	6.3244×10^{-6}	8.4582×10^{-6}	3.2049×10^{-5}	2.2690×10^{-5}
0.2	5.2199×10^{-6}	6.4582×10^{-6}	2.3143×10^{-5}	9.3914×10^{-5}
0.3	3.2434×10^{-6}	2.7291×10^{-6}	1.2999×10^{-5}	3.3777×10^{-4}
0.4	5.1239×10^{-6}	4.2598×10^{-6}	4.3305×10^{-5}	2.4709×10^{-5}
0.5	8.817×10^{-14}	5.0732×10^{-13}	2.9411×10^{-13}	6.6518×10^{-14}
0.6	7.9310×10^{-6}	6.9917×10^{-6}	4.9636×10^{-5}	3.7512×10^{-4}
0.7	3.7105×10^{-6}	3.0050×10^{-6}	2.2815×10^{-5}	2.3572×10^{-5}
0.8	6.3519×10^{-6}	2.5799×10^{-6}	1.0009×10^{-5}	3.601×10^{-4}
0.9	8.2091×10^{-6}	3.6408×10^{-6}	6.1586×10^{-5}	6.1890×10^{-4}
1.0	2.8069×10^{-6}	6.5559×10^{-6}	5.3071×10^{-5}	3.7142×10^{-5}

Piecewise Solutions for Example 2 with $N = 40, h = 0.05$ domain r $\in$ [0, 1]

$$Z(r,t) = \begin{cases} -4.63096\times10^{-21} + \mathrm{r}\left(1.99754 + \mathrm{r}\left(-0.0678009 + \left(1.27488 - 6.53823\,\mathrm{r}\right)r\right)\right), & r \in [0.0,\ 0.05) \\ -0.034288 + \mathrm{r}\left(2.69241 + \mathrm{r}\left(-5.00091 + \left(14.9866 - 16.862\,\mathrm{r}\right)r\right)\right), & r \in [0.05,\ 0.1) \\ -0.574781 + \mathrm{r}\left(8.18877 + \mathrm{r}\left(-24.6293 + \left(42.6022 - 27.6675\,\mathrm{r}\right)r\right)\right), & r \in [0.1,\ 0.15) \\ -3.23164 + \mathrm{r}\left(26.1606 + \mathrm{r}\left(-67.2561 + \left(82.2811 - 37.7756r\right)r\right)\right), & r \in [0.15,\ 0.2) \\ -11.2861 + \mathrm{r}\left(66.8943 + \mathrm{r}\left(-139.333 + \left(132.053 - 46.9537\,\mathrm{r}\right)r\right)\right), & r \in [0.2,\ 0.25) \\ -29.9023 + \mathrm{r}\left(141.887 + \mathrm{r}\left(-244.717 + \left(189.38 - 54.9758\,\mathrm{r}\right)r\right)\right), & r \in [0.25,\ 0.3) \\ -65.9339 + \mathrm{r}\left(262.164 + \mathrm{r}\left(-384.178 + \left(251.274 - 61.6441\,\mathrm{r}\right)r\right)\right), & r \in [0.3,\ 0.35) \\ -127.276 + \mathrm{r}\left(436.376 + \mathrm{r}\left(-555.071 + \left(314.407 - 66.7946\,\mathrm{r}\right)\right)\right) & r \in [0.35,\ 0.4) \\ -221.761 + \mathrm{r}\left(668.899 + \mathrm{r}\left(-751.178 + \left(375.237 - 70.3003\,\mathrm{r}\right)r\right)\right), & r \in [0.4,\ 0.45) \\ -355.635 + r\left(958.002 + \mathrm{r}\left(-962.771 + \left(430.145 - 72.0751\,\mathrm{r}\right)r\right)\right), & r \in [0.45,\ 0.5) \\ -531.719 + \mathrm{r}\left(1294.3 + \mathrm{r}\left(-1176.86 + \left(475.577 - 72.0751\,\mathrm{r}\right)r\right)\right), & r \in [0.5,\ 0.55) \\ -747.382 + \mathrm{r}\left(1659.58 + \mathrm{r}\left(-1377.67 + \left(508.183 - 70.3003\,\mathrm{r}\right)r\right)\right), & r \in [0.55,\ 0.6) \\ -992.505 + \mathrm{r}\left(2026.23 + \mathrm{r}\left(-1547.27 + \left(524.959 - 66.7946\,\mathrm{r}\right)r\right)\right), & r \in [0.6,\ 0.65) \\ -1247.64 + \mathrm{r}\left(2357.2 + \mathrm{r}\left(-1666.4 + \left(523.369 - 61.6441\,\mathrm{r}\right)\right)\right), & r \in [0.65,\ 0.7) \\ -1482.58 + \mathrm{r}\left(2606.78 + r\left(-1715.39 + \left(501.466 - 54.9758\,\mathrm{r}\right)r\right)\right), & r \in [0.7,\ 0.75) \\ -1655.55 + \mathrm{r}\left(2722.08 + \mathrm{r}\left(-1675.26 + \left(457.986 - 46.9537\,\mathrm{r}\right)r\right)\right), & r \in [0.75,\ 0.8) \\ -1713.29 + \mathrm{r}\left(2645.29 + \mathrm{r}\left(-1528.75 + \left(392.421 - 37.7756\,\mathrm{r}\right)r\right)\right), & r \in [0.8,\ 0.85) \\ -1592.06 + \mathrm{r}\left(2316.62 + \mathrm{r}\left(-1261.52 + \left(305.078 - 27.6675\,\mathrm{r}\right)r\right)\right), & r \in [0.85,\ 0.9) \\ -1218.77 + \mathrm{r}\left(1676.31 + \mathrm{r}\left(-862.284 + \left(196.908 - 16.862\,\mathrm{r}\right)r\right)\right), & r \in [0.9,\ 0.95) \\ -591.748 + \mathrm{r}\left(771.586 + r\left(-375.231 + \left(80.8869 - 6.53823\,\mathrm{r}\right)r\right)\right), & r \in [0.95,\ 1.0]. \end{cases}$$

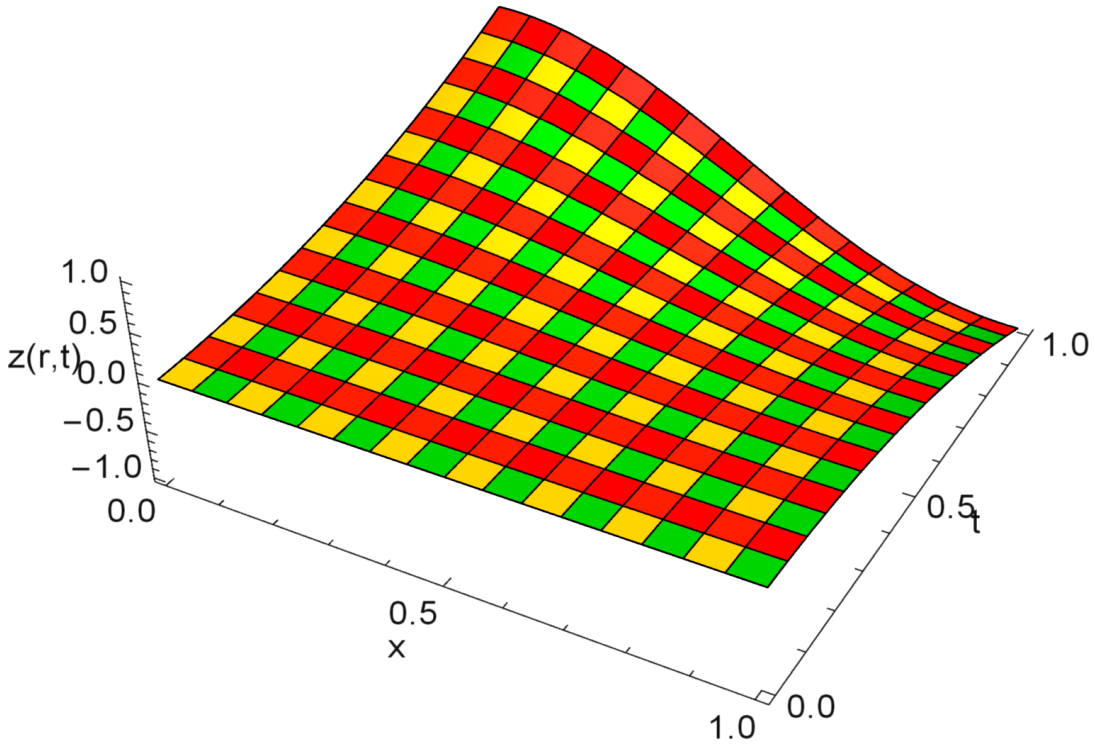

Figure 5 3D plot for the exact solution of Example 2 when $N = 40, \beta = 0.4$ **and** $\Delta t = 0.01$**.**

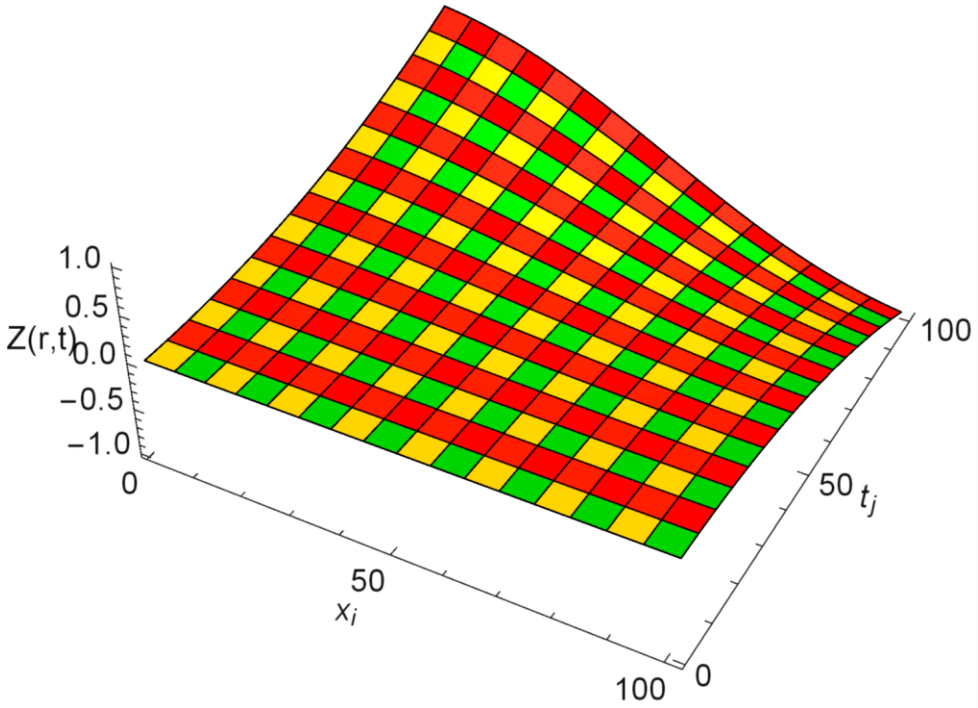

Figure 6 3 D plot for the approximate solution of Example 2 when $N = 40, \beta = 0.4$ **and** $\Delta t = 0.01$**.**

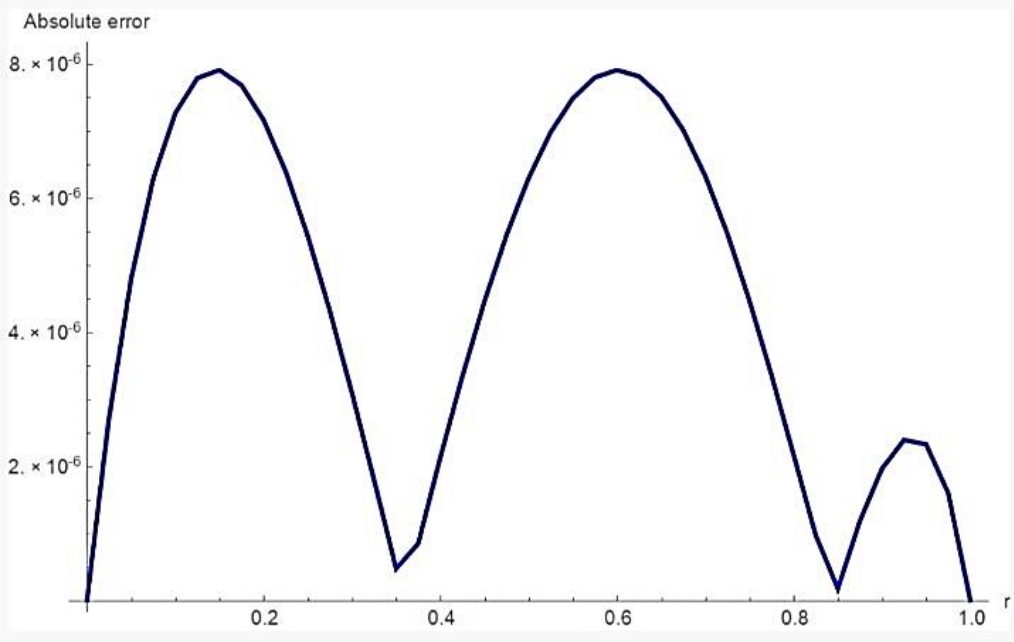

Figure 7 Absolute error when $N = 40, \beta = 0.4$ and $\Delta t = 0.01$ for Example 2.

Conclusion

Modeling with a non-integer order derivative is more accurate and reliable than the integer order scenario, according to research findings. An efficient approach for solving the time-fractional Burgers Equation is provided in this research article. The finite difference method has been utilized to discretize fractional derivative in Caputo sense. In the discretized version, singularity is absent. Using Taylor's series expansion, the Extended Cubic B-Spline approximation is constructed using a linear combination of its neighboring nodal values. The proposed approach is specifically designed for fractional partial differential equations (FPDEs) involving nonlinear second-order time derivatives. By increasing N and M, it can be observed that the error decrease. The E_X CBS method is shown to be unconditionally stable and convergent by both theoretical and computational results. Comparing this new approximation to earlier techniques covered in the literature, the results are more accurate. The paper includes a rigorous analysis of the stability and convergence of the proposed scheme. The applied method is un-conditionally stable and convergent.

References

[1] N. SUGIMOTO, "Generalized Burgers equations and fractional calculus," Nonlinear wave motion, pp. 162–179, 1989.

[2] N. Sugimoto, "Burgers equation with a fractional derivative; hereditary effects on nonlinear acoustic waves," J Fluid Mech, vol. 225, pp. 631–653, 1991.

[3] R. Garra, "Fractional-calculus model for temperature and pressure waves in fluid-saturated porous rocks," Physical Review E—Statistical, Nonlinear, and Soft Matter Physics, vol. 84, no. 3, p. 036605, 2011.

[4] J. J. Keller, "Propagation of simple non-linear waves in gas filled tubes with friction," Zeitschrift für angewandte Mathematik und Physik ZAMP, vol. 32, no. 2, pp. 170–181, 1981.

[5] V. D. Djordjevic and T. M. Atanackovic, "Similarity solutions to nonlinear heat conduction and Burgers/Korteweg–deVries fractional equations," J Comput Appl Math, vol. 222, no. 2, pp. 701–714, 2008.

[6] M. Inc, "The approximate and exact solutions of the space-and time-fractional Burgers equations with initial conditions by variational iteration method," J Math Anal Appl, vol. 345, no. 1, pp. 476–484, 2008.

[7] A. Esen and O. Tasbozan, "Numerical solution of time-fractional Burgers equation," Acta Univ Sapientiae Matem, vol. 7, no. 2, pp. 167–185, 2015.

[8] S. S. Siddiqi and S. Arshed, "Numerical solution of time-fractional fourth-order partial differential equations," Int J Comput Math, vol. 92, no. 7, pp. 1496–1518, 2015.

[9] A. Mohebbi, "Analysis of a numerical method for the solution of time-fractional Burgers equation," Bulletin of the Iranian Mathematical Society, vol. 44, pp. 457–480, 2018.

[10] N. A. Asif, Z. Hammouch, M. B. Riaz, and H. Bulut, "Analytical solution of a Maxwell fluid with slip effects in view of the Caputo-Fabrizio derivative⋆," The European Physical Journal Plus, vol. 133, pp. 1–13, 2018.

[11] F. Liu, P. Zhuang, V. Anh, I. Turner, and K. Burrage, "Stability and convergence of the difference methods for the space–time-fractional advection–diffusion equation," Appl Math Comput, vol. 191, no. 1, pp. 12–20, 2007.

[12] S. G. Rubin and R. A. Graves Jr, "A cubic spline approximation for problems in fluid mechanics," 1975.

[13] X.-L. Han and S.-J. Liu, "An extension of the cubic uniform B-Spline curves," Journal of Computer Aided Design and Computer Graphics, vol. 15, no. 5, pp. 576–578, 2003.

[14] M. Hashemi, M. Inc, E. Karatas, and A. Akgul, "A numerical investigation on Burgers equation by MOL-GPS method," Journal of Advanced Physics, vol. 6, no. 3, 2017.

[15] L. Song and H. Zhang, "Application of homotopy analysis method to fractional KdV–Burgers–Kuramoto equation," Phys Lett A, vol. 367, no. 1–2, pp. 88–94, 2007.

[16] J. Liu and G. Hou, "Numerical solutions of the space-and time-fractional coupled Burgers equations by generalized differential transform method," Appl Math Comput, vol. 217, no. 16, pp. 7001–7008, 2011.

[17] B. Lombard, D. Matignon, and Y. Le Gorrec, "A fractional Burgers equation arising in nonlinear acoustics: theory and numerics," IFAC Proceedings Volumes, vol. 46, no. 23, pp. 406–411, 2013.

[18] B. Lombard, D. Matignon, and Y. Le Gorrec, "A fractional Burgers equation arising in nonlinear acoustics: theory and numerics," IFAC Proceedings Volumes, vol. 46, no. 23, pp. 406–411, 2013.

[19] K. M. Saad and E. H. F. Al-Sharif, "Analytical study for time and time-space fractional Burgers equation," Adv Differ Equ, vol. 2017, pp. 1–15, 2017.

[20] A. Yokus and D. Kaya, "Numerical and exact solutions for time-fractional Burgers equation," 2017.

[21] A. Esen and O. Tasbozan, "Numerical solution of time-fractional Burgers equation by cubic B-Spline finite elements," Mediterranean Journal of Mathematics, vol. 13, pp. 1325–1337, 2016.

[22] A. Atangana and Z. Hammouch, "Fractional calculus with power law: The cradle of our ancestors⋆," The European Physical Journal Plus, vol. 134, no. 9, p. 429, 2019.

[23] S. T. Mohyud-Din, T. Akram, M. Abbas, A. I. Ismail, and N. H. M. Ali, "A fully implicit finite difference scheme based on extended cubic B-Splines for time-fractional advection–diffusion equation," Adv Differ Equ, vol. 2018, pp. 1–17, 2018.

[24] M. M. Ghalib, A. A. Zafar, M. B. Riaz, Z. Hammouch, and K. Shabbir, "Analytical approach for the steady MHD conjugate viscous fluid flow in a porous medium with nonsingular fractional derivative," Physica A: Statistical Mechanics and its Applications, vol. 554, p. 123941, 2020.

[25] T. Akram, M. Abbas, and A. I. Ismail, "Numerical solution of fractional cable equation via extended cubic B-Spline," in AIP Conference Proceedings, AIP Publishing, 2019.

[26] M. Yaseen and M. Abbas, "An efficient computational technique based on cubic trigonometric B-Splines for time-fractional Burgers equation," Int J Comput Math, vol. 97, no. 3, pp. 725–738, 2020.

[27] C. A. Hall, "On error bounds for spline interpolation," J Approx Theory, vol. 1, no. 2, pp. 209–218, 1968.

[28] C. de Boor, "On the convergence of odd-degree spline interpolation," J Approx Theory, vol. 1, no. 4, pp. 452–463, 1968.

[29] A. Usman, M. Amin, S. Hassan, and J. Kousar, "NUMERICAL TREATMENT OF TIME-FRACTIONAL ADVECTION DIFFUSION EQUATION VIA B-SPLINE COLLOCATION APPROACH," Kashf Journal of Multidisciplinary Research, vol. 2, no. 07, pp. 25–50, 2025.

[30] S. Hassan, M. Amin, and S. Mushtaq, "APPLICATION OF A HYBRID B-SPLINE METHOD FOR THE NUMERICAL ANALYSIS OF TIME-FRACTIONAL DIFFUSION WAVE EQUATION," Kashf Journal of Multidisciplinary Research, vol. 2, no. 06, pp. 104–126, 2025.

[31] M. Waqas, M. Amin, and S. Mushtaq, "AN EFFICIENT HYBRID B-SPLINE APPROACH FOR NUMERICAL APPROXIMATION OF TIME-FRACTIONAL TELEGRAPH EQUATIONS," Center for Management Science Research, vol. 3, no. 3, pp. 992–1011, 2025.

[32] A. S. Heilat, N. N. A. Hamid, and A. I. M. Ismail, "Extended cubic B-Spline method for solving a linear system of second-order boundary value problems," Springerplus, vol. 5, no. 1, p. 1314, 2016.

[33] K. M. Owolabi and Z. Hammouch, "Mathematical modeling and analysis of two-variable system with noninteger-order derivative," Chaos: An Interdisciplinary Journal of Nonlinear Science, vol. 29, no. 1, 2019.

[34] S. T. Mohyud-Din, T. Akram, M. Abbas, A. I. Ismail, and N. H. M. Ali, "A fully implicit finite difference scheme based on extended cubic B-Splines for time-fractional advection–diffusion equation," Adv Differ Equ, vol. 2018, pp. 1–17, 201